Oxidation of nitric oxide by oxomanganese–salen complexes: a new mechanism for cellular protection by superoxide dismutase/catalase mimetics

Martyn A. SHARPE[1], Richard OLLOSSON, Victoria C. STEWART and John B. CLARK

Department of Molecular Pathogenesis, Division of Neurochemistry, Institute of Neurology, University College London, Queen Square, London WC1N 3BG, U.K.

Manganese–salen complexes (Mn-Salen), including EUK-8 [manganese *N*,*N*′-bis(salicylidene)ethylenediamine chloride] and EUK-134 [manganese 3-methoxy *N*,*N*′-bis(salicylidene)ethylenediamine chloride], have been reported to possess combined superoxide dismutase (SOD) and catalase mimetic functions. Because of this SOD/catalase mimicry, EUK-8 and EUK-134 have been investigated as possible therapeutic agents in neurological disorders resulting from oxidative stress, including Alzheimer's disease, Parkinson's disease, stroke and multiple sclerosis. These actions have been explained by the ability of the Mn-Salen to remove deleterious superoxide (O_2^-) and H_2O_2. However, in addition to oxidative stress, cells in models for neurodegenerative diseases may also be subjected to damage from reactive nitrogen oxides (nitrosative stress), resulting from elevated levels of NO and sister compounds, including peroxynitrite ($ONOO^-$). We have been examining the interaction of EUK-8 and EUK-134 with NO and $ONOO^-$. We find that in the presence of a per-species (H_2O_2, $ONOO^-$, peracetate and persulphate), the Mn-Salen complexes are oxidized to the corresponding oxo-species (oxoMn-Salen). OxoMn-Salens are potent oxidants, and we demonstrate that they can rapidly oxidize NO to NO_2 and also oxidize nitrite (NO_2^- to nitrate (NO_2^-). Thus these Mn-Salens have the potential to ameliorate cellular damage caused by both oxidative and nitrosative stresses, by the catalytic breakdown of O_2^-, H_2O_2, $ONOO^-$ and NO to benign species: O_2, H_2O, NO_2^- and NO_3^-.

Key words: neurodegenerative, nitrosative stress, oxidative stress, peroxynitrite, sepsis.

INTRODUCTION

In 1996, Harman proposed the 'free radical theory of aging' [1], which implicated an increase in the steady-state levels of oxidatively damaged biomolecules due to reactive oxygen species including superoxide (O_2^-), H_2O_2 and (in the presence of transition metal ions) hydroxyl radical ($OH^\bullet$). Mammals have three enzymes to dismutate O_2^- into O_2 and H_2O_2; two Cu/Zn superoxide dismutases (SODs), one cytosolic and the other extracellular, and a mitochondrial MnSOD. H_2O_2 is detoxified either to water and O_2 by catalase or to water by glutathione peroxidase. Several lines of evidence have supported Harman's theory (for a review, see [2]). (i) Life expectancy declines with an increase in the generation of O_2^- or H_2O_2, in many species [3,4] and in organisms with low levels of SOD [5] and catalase [6]. (ii) Life expectancy of *Drosophila* can be extended by up to one-third in mutants overexpressing both SOD and catalase [7]. The overexpression of SOD and catalase in these flies ameliorated the age-related accumulation of molecular oxidative damage and increased their resistance to acute oxidative stress.

Recently it has been shown that artificial SOD/catalase mimics [8] are able to increase the life span of nematodes by up to 50% [9]. These mimetics belong to a group called the manganese–salen complexes [Mn-Salens; where H_2 Salen is *N*,*N*′-bis(salicylidene)-ethylenediamine]. Their biological activity has been examined, in association with a pharmaceutical company (Eukarion, Bedford, MA, U.S.A.), and has been shown to protect cells from oxidative stress in a large number of disease models, including Alzheimer's disease [10], Parkinson's disease [11], stroke [12], motor neuron disease [13], multiple sclerosis [14], excitotoxic neuronal injury [15] and ischaemia/reperfusion in both heart and kidney tissue [16,17]. The structure of Mn-Salen complexes is shown in Figure 1.

The mechanism for the dismutation of O_2^- involves the reduction of Mn(III) to Mn(II) by O_2^-, which is oxidized to O_2 (eqn 1). This Mn(II) is subsequently oxidized back to Mn(III) by another molecule of O_2^-, yielding H_2O_2 (eqn 2). This mechanism is very similar to that of MnSOD [18].

$$Mn(III) + O_2^- \rightarrow Mn(II) + O_2 \quad (1)$$

$$2H^+ + Mn(II) + O_2^- \rightarrow Mn(III) + H_2O_2 \quad (2)$$

The mechanism by which the Mn-Salen acts as a catalase mimetic involves the oxidation of Mn-Salen to an oxomanganese–salen complex (oxoMn-Salen) by H_2O_2, releasing water (eqn 3). The oxoMn-Salen is then reduced by another molecule of H_2O_2 to regenerate the Mn-Salen and generate water and O_2 (eqn 4).

$$Mn(III) + H_2O_2 \rightarrow Mn(V)O^{2-} + H_2O \quad (3)$$

$$Mn(V)O^{2-} + H_2O_2 \rightarrow Mn(III) + H_2O + O_2 \quad (4)$$

OxoMn-Salen complexes are powerful oxidants and have a wide range of uses in inorganic/organic synthesis (for a review, see [19]). In this role, oxoMn-Salens are generated from Mn-Salens using a number of atomic-oxygen-donating species, including H_2O_2, but normally employing iodosylbenzene or hypochlorite (OCl^-) [20]. Neutrophils contain the enzymes myeloperoxidase and eosinophil peroxidase, which catalyse the reaction of H_2O_2 with Cl^- to generate OCl^- [21]. OCl^- has been implicated as an

Abbreviations used: C-PTIO, 2-(4-carboxyphenyl)-4,4,5,5-tetramethylimidazoline 1-oxyl 3-oxide; DTPA, diethylenetriaminepenta-acetic acid; IFN-γ, interferon-γ; LPS, lipopolysaccharide; Mn-Salen, manganese–salen complex; MEM, minimal essential medium; OCl^-, hypochlorite; $ONOO^-$, peroxynitrite; oxoMn-Salen, oxomanganese–salen complex; SOD, superoxide dismutase; EUK-8, manganese *N*,*N*′-bis(salicylidene)ethylenediamine chloride; EUK-134, manganese 3-methoxy-*N*,*N*′-bis(salicylidene)ethylenediamine chloride.

[1] To whom correspondence should be addressed (e-mail msharpe@ion.ucl.ac.uk).

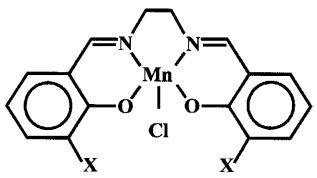

Figure 1 The structure of Mn-Salens

In EUK-8, X is H; in EUK-134, X is OCH_3.

agent causing oxidative stress in a number of disease states and has been shown to damage endothelial cells [22].

In addition to oxidative stress, cells also face nitrosative stresses from certain nitrogen oxides, in both age and disease. NO is a free radical that has a key role in both normal physiological processes and disease states (for a general review, see [23]; for a review about NO and the brain, see [24]). NO reacts with O_2^- [25] at a rate approaching the diffusion barrier, generating peroxynitrite ($ONOO^-$). $ONOO^-$ is also generated rapidly from the reaction of nitroxyl anion (NO^-) and O_2. NO^- is generated from NO, by mitochondria, by two distinct reductants: ferrocytochrome *c* [26] and ubiquinol [27].

$ONOO^-$ has a half-life of approx. 1 s under physiological conditions, i.e. in the presence of CO_2 [28]. $ONOO^-$ oxidizes protein and non-protein thiols [29] and methionine [30]. $ONOO^-$ is also capable of nitrosylating (addition of NO) and nitrating (addition of NO_2) a large number of compounds, including amino acids; the nitration of tyrosine by $ONOO^-$ occurs *in vitro* and *in vivo* and is now well understood [31].

Increased levels of nitrotyrosine, a marker of steady-state $ONOO^-$ levels, have been observed in aging mammalian tissues, including the white matter of monkey brain [32], rat cerebral cortex [33], rat aorta [34] and human cerebrospinal fluid [35]. In addition, serum nitrate (the major product of $ONOO^-$ breakdown) has been shown to increase in human serum in an age-dependent manner [36].

Nitrosative stress has also been implicated in a number of disease states in brain (for a review, see [37]), which have benefitted from treatment with Mn-Salen, including Alzheimer's disease (for a review, see [38]), Parkinson's disease [39], stroke [40], motor neuron disease [41] and multiple sclerosis [42]. With this in mind we have examined the chemistry of Mn-Salen with respect to NO and $ONOO^-$.

EXPERIMENTAL

Preparation of Mn-Salen

Mn-Salens are relatively easy to prepare and to purify. Manganese *N*,*N*′-bis(salicylidene)ethylenediamine chloride (EUK-8) and manganese 3-methoxy-*N*,*N*′-bis(salicylidene)ethylenediamine chloride (EUK-134) were prepared according to the procedure of Baker et al. [12], based on that of Boucher and Farrell [43,44]. The bis(salicylaldehyde)ethylenediamine-substituted ligands were prepared by the addition of 50 ml of 200 mM ethylenediamine to an equal volume of 400 mM of the substituted aldehyde (salicylaldehyde for EUK-8 and *o*-vanillin for EUK-134) in 100 % ethanol. The precipitate was filtered, washed with 100 % ethanol and air-dried. Solid Mn(II) acetate tetrahydrate was added to a stirred suspension of 30 mM ligand (in 95 % ethanol) to a final concentration of 30 mM and refluxed for 1 h. The dark-brown solutions were dried under a stream of air. The crude product, a brown solid, was washed with acetone, filtered and air-dried. These acetate complexes were converted into the corresponding chlorides through treatment of an aqueous solution (final concentration, 100 mM) of the Mn-Salen acetate, warmed to 50 °C, with 500 mM KCl. The suspension was cooled in an ice/water bath and then filtered; the brown solid was washed with water and acetone. The concentrations of the Mn-Salen were determined from the absorption spectra in absolute ethanol, as in [43].

Preparation of NO

NO solutions were prepared as described previously [26], by the addition of 2 M H_2SO_4 to solid $NaNO_2$ in a Kipps apparatus. The NO gas was passed through three NaOH (20 %) traps to remove NO_2, dried by passage through solid NaOH and then through a solid-CO_2 trap. The gas was collected in water that had undergone four vacuum/N_2 deoxygenation cycles.

Measurement of O_2 and NO

NO concentration was measured using a World Precision Instruments (WPI) ISO-200 NO electrode connected to a WPI ISO-NO Mark I NO meter. The data were collected via a PowerLab/800 (ADInstruments) data-collection interface. The electrode was placed in a 1 ml thermostatically jacketed glass reaction chamber, which also housed a Clark-type O_2 electrode (Rank Bros, Bottisham, Cambs., U.K.). The NO electrode was calibrated by filling the reaction chamber with KI/H_2SO_4 (0.1 M) and titrating with stock solutions of NO_2^-.

Optical spectroscopy

Spectra were recorded at room temperature using a Hewlett–Packard 8453 diode array spectrophotometer.

Measurement of NO_2^-/NO_3^-

Nitrite was assayed using the Griess reaction, and nitrate was assayed either by the nitrate reductase method of Green et al. [45] or the V(III) method of Miranda et al. [46]. Samples or standards of 100 μl were added to 50 μl of 2 % (w/v) sulphanilamide in 5 % (v/v) HCl and 50 μl of 0.1 % naphthylethylenediamine hydrochloride in a 96-well plate (Nunc, Roskilde, Denmark). The absorbance, after 30 min of incubation, was recorded at 540 nm, using a SpectromaxPlus absorbance spectrophotometer (Molecular Devices).

Preparation of $ONOO^-$

$ONOO^-$ was prepared from amyl nitrite and H_2O_2 using the method of Uppu and Pryor [47]. Amyl nitrite was washed three times and 26 ml was added to 100 ml of 2 M H_2O_2, 2 M NaOH and 2 mM diethylenetriaminepenta-acetic acid (DTPA). This solution was stirred vigorously for 3 h at 4 °C. The lower aqueous layer was removed from the organic phase using a separating funnel and washed three times with an equal volume of ice-cold hexane. To remove residual H_2O_2, activated MnO_2 was added gradually to the $ONOO^-$. The solution was aliquoted into Eppendorf tubes and stored at 200 K. After thawing, the $ONOO^-$ solutions were centrifuged to pellet MnO_2.

The concentration of $ONOO^-$ was determined spectrophotometrically using an absorption coefficient of 1670 M^{-1} at 302 nm, in 100 mM NaOH.

Cell culture

Primary cortical astrocyte cultures were prepared from neonatal Wistar rats (1–2 days old) as described by Bolaños et al. [48]. Cell suspensions were plated at a density of 1×10^5 cells $\cdot$ cm^{-2} in 80 cm^2 flasks and were cultured for 7 days in D-valine-based minimal essential medium (MEM) supplemented with 10 % (v/v) fetal bovine serum and 2 mM L-glutamine to minimize fibroblast growth. Cells were then cultured for another 7 days in L-valine-based MEM. Cultures showed 90–95 % immunopositivity against glial fibrillary acidic protein. Astrocytes were then seeded at a density of 1×10^5 cells $\cdot$ cm^{-2} in six-well culture dishes and used for experiments after 24 h.

Cells were treated with interferon-γ (IFN-γ; 100 units $\cdot$ ml^{-1}) + lipopolysaccharide (LPS; 1 μg $\cdot$ ml^{-1}) or EUK-8 or EUK-134 (50 μM) for 24 h in Phenol Red-free, serum-free MEM. In addition, some cells were treated with a combination of either EUK-8 or EUK-134 and IFN-γ/LPS for 24 h. Some wells were left untreated. At the end of incubation period, the cell culture medium was collected and the cells were trypsinized and pelleted. The cell culture medium was analysed for nitrite and nitrate. The cell pellets were resuspended in respiration buffer (134.2 mM NaCl, 20 mM glucose, 20 mM Hepes, 5.3 mM KCl, 4.1 mM $NaHCO_3$, 2 mM $CaCl_2$, 0.43 mM KH_2PO_4 and 0.33 mM Na_2HPO_4, pH 7.4). Cell viability was assessed by Trypan Blue exclusion at the end of each incubation and found to be unaffected by the treatments.

Reagents

Bovine liver catalase was obtained from Boehringer Mannheim, rat recombinant IFN-γ was obtained from Calbiochem, LPS (*Escherichia coli* 026:Bb), fetal bovine serum, MEM and tissue-culture plastics were purchased from Life Technologies, and other reagents were obtained from Sigma–Aldrich, who now also supply bis(salicylaldehyde)ethylenediamine.

RESULTS

Oxidation of EUK-8 by peroxides and OCl$^-$

Figure 2 (top panel) shows the aqueous absorbance spectra of EUK-8 and oxoEUK-8 at neutral pH. Conversion of Mn-Salen into the oxo-species is accompanied by a change in the spectrum. Figure 2 (bottom panel) shows the effect of various atomic-oxygen-donating compounds on the difference spectra of 50 μM EUK-8. Persulphate, peracetate, H_2O_2 and ONOO$^-$ were all capable of acting as atomic oxygen donors to EUK-8 and EUK-134 and generating the same spectral species as OCl$^-$. This strongly suggests that Mn-Salen may be able to act therapeutically in the detoxification of excessive ONOO$^-$ and OCl$^-$. The reason that lower levels of oxoEUK-8 were generated in the presence of H_2O_2, compared with the other atomic-oxygen-donating reagents, is due to the catalase-like activity of EUK-8. Although H_2O_2 generates the oxo-species (eqn 3), it also consumes it (eqn 4). It was found that 1 mM H_2O_2 was the optimal concentration to add to 50 μM EUK-8 to generate the greatest level of the oxo-species, within the measured time frame.

Catalase mimicry of EUK-8

We examined the kinetics of EUK-8's catalase-mimetic mode of action at neutral pH and 37 °C. Although EUK-8 does have some catalase-like activity, as reported by Baker et al. [12], it is very much less active than catalase under the same conditions (Figure 3, top panel). The second-order rate constant for EUK-8 was only approx. 8.3 $M^{-1} \cdot s^{-1}$ (Figure 3, bottom panel) and for EUK-134 was approx. 30 $M^{-1} \cdot s^{-1}$, approximately twice the values determined at 25 °C by Baker et al. [12]. These values compare with the rate for mammalian catalase of $> 10^7$ $M^{-1} \cdot s^{-1}$ under similar conditions. This difference in the rates of H_2O_2 consumption by these mimetics and the enzyme present *in vivo* raises the possibility that the catalase-like activity of Mn-Salen complexes may not be their major cytoprotective action.

Effect of EUK-134 and oxoEUK-134 on NO

We examined the stability of NO in the presence and absence of EUK-134, prior to and following the addition of H_2O_2, measuring both NO and O_2 polarographically (Figure 4, top panel). Initially, H_2O_2 was added to the chamber to a final concentration of 200 μM and this was followed by an aliquot of NO (final concentration, 6 μM). The addition of NO caused a rapid rise in the NO signal, which was followed by a slow decay, as the NO oxidized away. This autoxidation of NO was basically unaffected by the presence of H_2O_2, when compared with the H_2O_2-free buffer, as in [49], although H_2O_2 slowly generated O_2 (Figure 4, top panel, lower trace).

After the decay of the first pulse of NO, EUK-134 was added to the H_2O_2-containing buffer to a final concentration of 200 μM, immediately followed by another addition of NO. In the presence of both H_2O_2 and Mn-Salen, NO is rapidly consumed. The insert shows the decay of NO in the presence of EUK-134, but in the absence of H_2O_2, on the same scale as the main NO trace. Hence, the decay of NO is the same as found in buffer, in the presence of Mn-Salen alone or H_2O_2 alone, but very rapid in the presence of Mn-Salen and H_2O_2 together.

Following the decay of the second addition of NO and the catalytic exhaustion of H_2O_2, a third aliquot of NO was added to the chamber. This time the NO had a slightly accelerated decay compared with the control.

Figure 4 (bottom panel) is an expanded view of Figure 4 (top panel) at the point where EUK-134 and NO were added to the H_2O_2 solution. It can be seen that the addition of NO prevented the production of O_2 by H_2O_2/EUK-134.

The interaction of H_2O_2, NO and Mn-Salen is similar to that seen in the presence of catalase [49], with the major difference being that, unlike catalase, NO does not bind to the metal centre. Figure 4 suggests that NO is incapable of reacting with Mn-Salen, but can rapidly react with oxoMn-Salen. This would suggest that the oxoMn-Salen is acting in a similar way to the ferryl group of compound II of catalase, another atomic oxygen donor. This was tested by generating oxoEUK-134 from another important pathogenic oxidant, ONOO$^-$, an oxidant with a short half-life in this buffering system (approx. 2 s). We examined whether ONOO$^-$-treated EUK-134 could also react with NO. Figure 5 (top panel) demonstrates that oxoEUK-134, generated by the addition of ONOO$^-$ to EUK-134, is capable of oxidizing NO. Here, as in Figure 4 (top panel), it can be seen that NO decays slowly in buffer (first NO addition). Addition of ONOO$^-$ to EUK-134 has no effect on the NO trace; the apparent oxygen generation appears to be due to the addition of ice-cold ONOO$^-$ to the buffer. A similar consumption of NO was observed using ONOO$^-$ and EUK-8.

The formation of oxoEUK-8 was investigated using optical spectroscopy, measured using the 440–800 nm wavepair (Figure 5, bottom panel). The lower traces show the ONOO$^-$-induced formation and decay of oxoEUK-8 in the presence and absence of NO. The spontaneous decay rate of oxoEUK-8 was 0.036 ± 0.0034 s^{-1} ($n = 5$) and almost doubled in the presence of 8 μM NO to 0.067 ± 0.0074 s^{-1} ($n = 5$), indicating a second-order

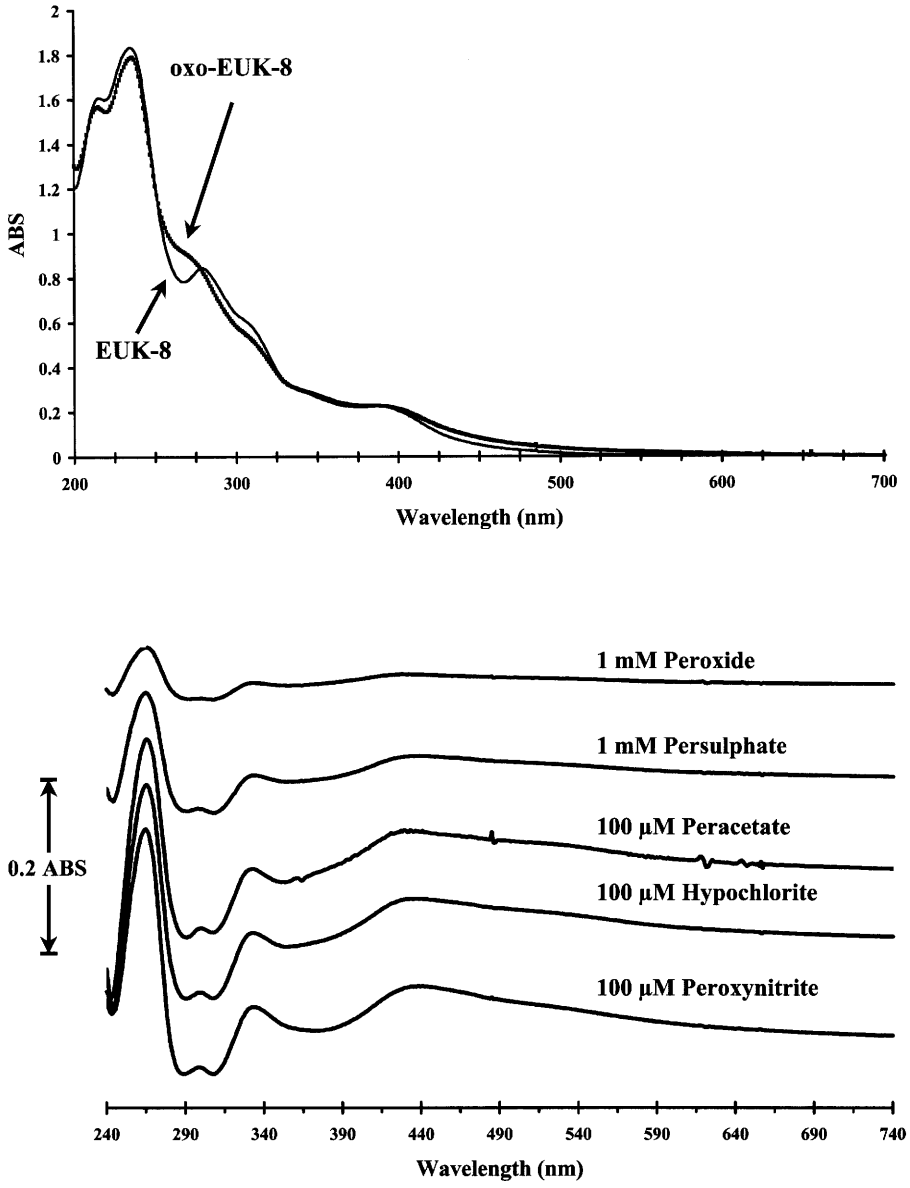

Figure 2 The absorbance spectrum of Mn-Salen and oxoMn-Salen

Top panel: absorbance spectrum of 50 μM EUK-8 and oxoEUK-8 in 100 mM potassium phosphate/20 μM DTPA, pH 7.0. The oxoEUK-8 spectrum was generated approx. 30 s after the addition of NaOCl (final concentration, 100 μM). Bottom panel: effect of various atomic-oxygen-donating compounds on the difference spectra of 50 μM EUK-8 in 100 mM potassium phosphate/20 μM DTPA, pH 7.0. The spectra were recorded approx. 30 s after addition of the oxidant.

rate constant of approx. 4×10^3 $M^{-1} \cdot s^{-1}$. The upper trace in Figure 5 (bottom panel) shows the difference in oxoEUK-8 concentration in the two traces and is indicative of the amount of oxoEUK-8 consumed by 8 μM NO. The average stoichiometry for the consumption of the oxoEUK-8 by NO was 0.84:1 ($n = 5$).

In similar experiments examining the decay of oxoEUK-134 (utilizing the 455–800 nm, wavepair) it was found that the decay rate was essentially identical with that of oxoEUK-8 at 0.036 ± 0.0017 s^{-1} ($n = 5$). The decay of oxoEUK-134 in the presence of 8 μM NO was approximately twice that of oxoEUK-8, at 0.1224 ± 0.0087 s^{-1} ($n = 5$). The average stoichiometry for the consumption of the oxoEUK-134 by NO was 0.67:1 ($n = 5$), This stoichiometry suggests that one molecule of NO is oxidized by one molecule of oxoMn-Salen.

Figure 5 (bottom panel) shows that the rate of oxoEUK-8 formation by $ONOO^-$ occurs within a few seconds, during which time $ONOO^-$ itself decays away. Because of the short half-life of $ONOO^-$ it is difficult to estimate accurately the rate constant for the reaction of $ONOO^-$ and Mn-Salen. From a number of experiments of the type shown in Figure 5 (bottom panel) the second-order rate constant for the reaction of $ONOO^-$ and EUK-8 or EUK-134 was calculated to be between 5×10^3 and 2×10^4 $M^{-1} \cdot s^{-1}$.

Effect of Mn-Salen and oxoMn-Salen on NO_2^-

We wished to examine the products of the decay of NO in the presence of oxoMn-Salen, and therefore assayed the solutions for

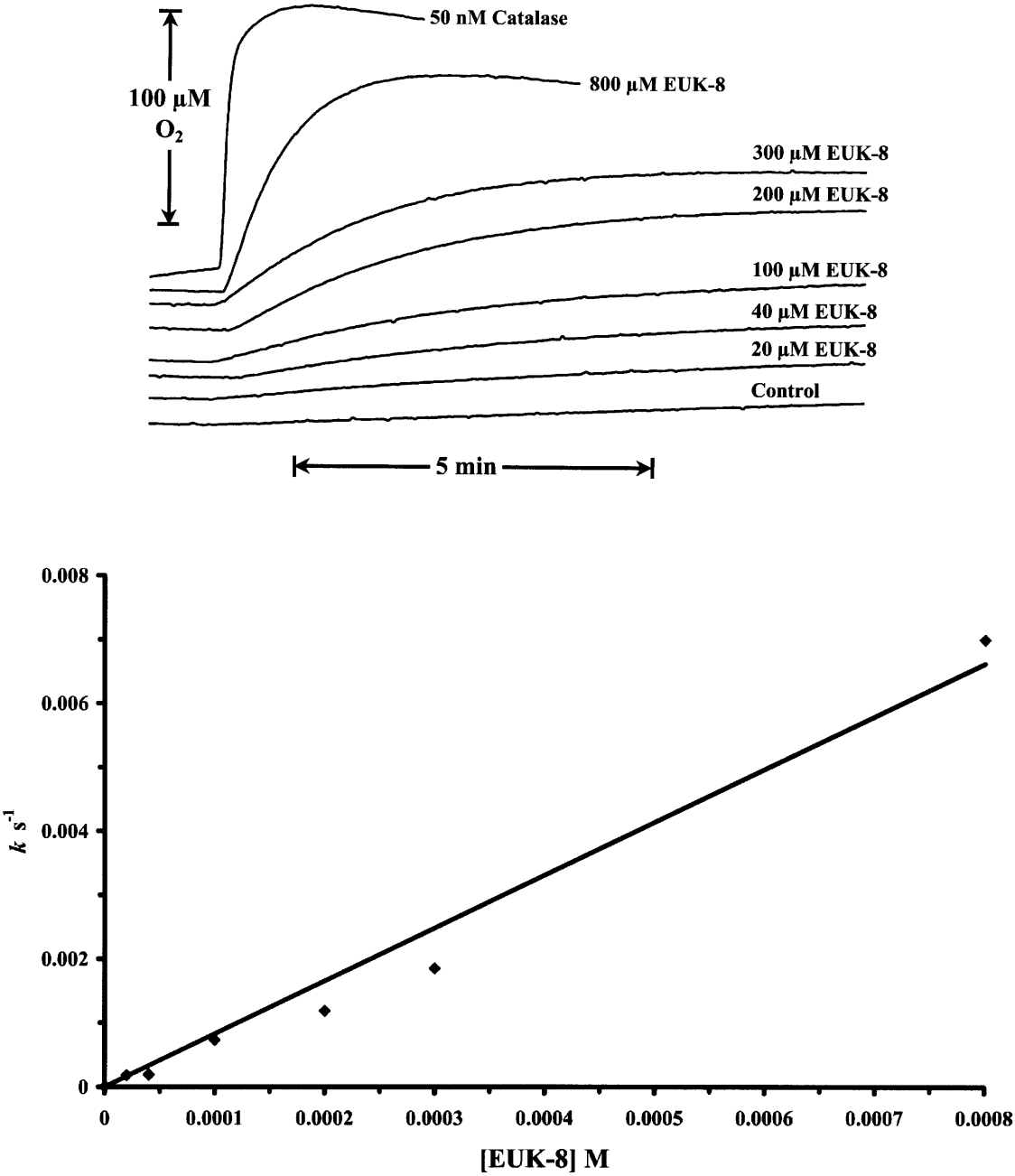

Figure 3 Catalase-mimetic action of EUK-8

Top panel: effect of different concentrations of EUK-8 on the generation of oxygen from H_2O_2. Various concentrations of EUK-8 were incubated in 100 mM potassium phosphate/20 μM DTPA, pH 7.0, at 37 °C in a glass chamber containing a Clark-type oxygen electrode. Following stabilization of the baseline, H_2O_2 was added to a final concentration of 250 μM. The EUK-8 catalysis was compared with that of 50 nM bovine liver catalase. Bottom panel: initial rates of oxygen production plotted against EUK-8 concentration, allowing the second-order rate constant for EUK-8 of 8.3 $M^{-1} \cdot s^{-1}$ to be calculated.

both nitrite and nitrate using the Griess reaction and the nitrate reductase method of Green et al. [45]. Upon assaying the products of the decay of NO, the levels of NO_2^-/NO_3^- were less than the amount of NO added. We therefore examined the effects of Mn-Salen and oxoMn-Salen on NO_2^- in buffer. Mn-Salen had no effect on NO_2^- concentrations when determined by the Griess assay. It was found that both oxoEUK-134 and oxoEUK-8 were capable of consuming NO_2^-.

Figure 6 shows the effect of H_2O_2 concentration on the measurement of 100 μM NO_2^- in the presence of 200 μM EUK-134 after 30 min of incubation. It can be seen that NO_2^- is consumed in the presence of oxoMn-Salen, but not Mn-Salen (i.e. see Figure 6 in the absence of H_2O_2). Control experiments, in which 50 nM catalase was added at the end of the incubation period, showed that trace levels of H_2O_2 were not interfering with the Greiss assay.

It was found that both Mn-Salens inhibited the reduction of NO_3^- to NO_2^- [45] by nitrate reductase and interfered with the conversion by V(III) [46] at the concentrations present in these assays. Using chemiluminesence determination of NO_2^-/NO_3^-

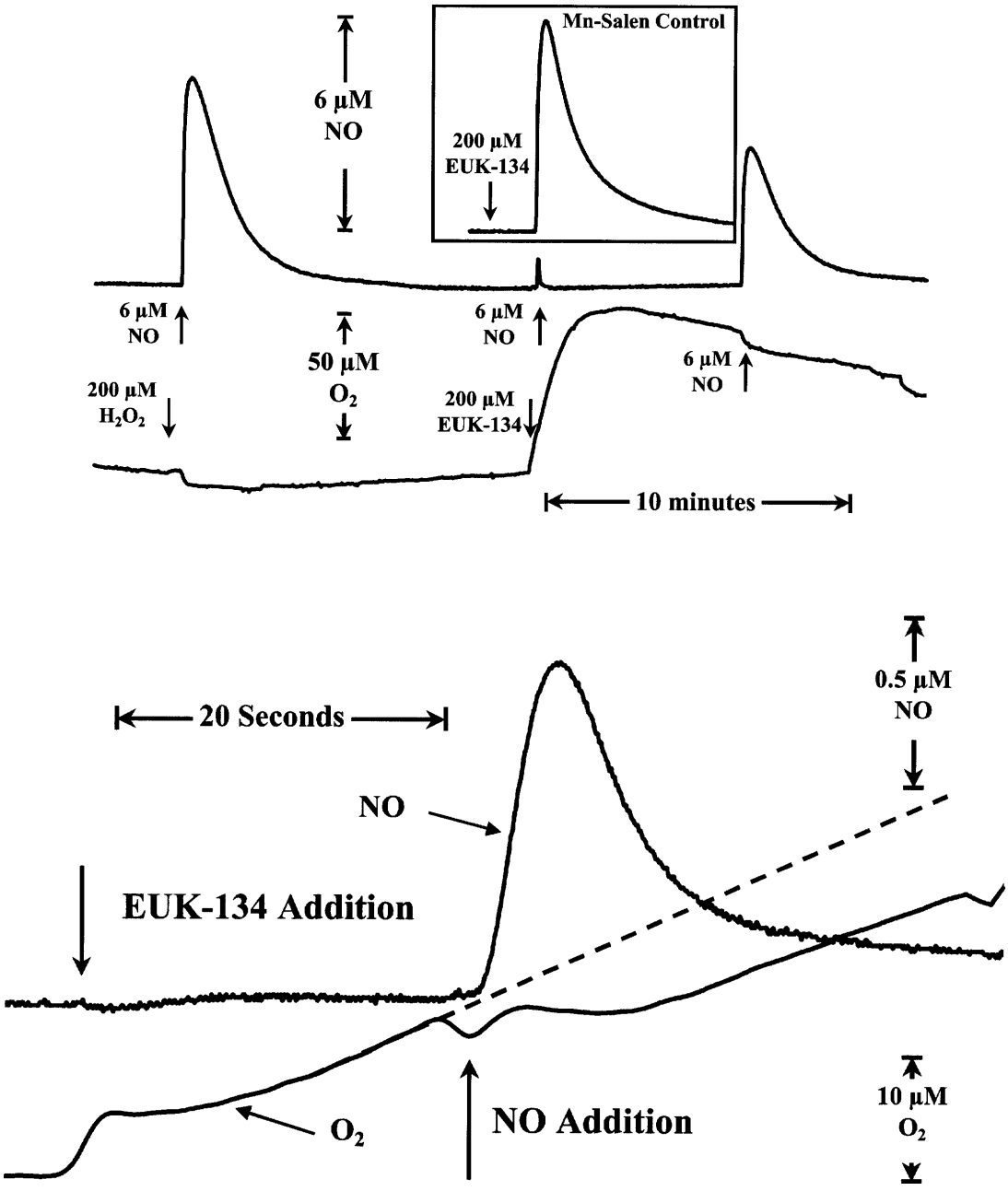

Figure 4 Effect of H_2O_2 and EUK-134 on the decay of NO

Top panel: a pair of NO and O_2 traces, recorded simultaneously. A 800 μl solution containing 100 mM potassium phosphate/20 μM DTPA, pH 7.0, at 37 °C was placed in a glass reaction chamber containing both an oxygen and an NO polarographic electrode. H_2O_2 was added to the chamber followed by NO, at final concentrations of 200 and 6 μM respectively. Following the decay of NO, 200 nmol · ml^{-1} EUK-134 was added, followed immediately by another aliquot of NO. Following the decay of the added NO and the catalytic exhaustion of H_2O_2, a final aliquot of NO was added to the chamber. The insert shows the action of 200 nmol · ml^{-1} EUK-134 on the decay of NO, in the absence of H_2O_2. The scales of the insert are the same as for the main trace. Bottom panel: on an expanded scale, the same data immediately following the addition of the second addition of NO in the top panel.

levels where Cd was used to convert NO_3^- into NO_2^- we were able to conclude that oxoMn-Salen acts as an atomic oxygen donor to NO_2^-, generating NO_3^-.

Effect of Mn-Salen-treated astrocytes on NO generation and decay

Figure 7 (top panel) shows the effect of EUK-8 (placed in the cells' growth media for 24 h prior to harvesting) on the ability of astrocytes to generate NO in the presence of inflammatory cytokines. The lower trace of Figure 7 (top panel) shows that control astrocytes, not treated with inflammatory cytokines, were incapable of generating NO, even in the presence of 50 μM arginine (the limiting substrate of inducible nitric oxide synthase).

Astrocytes treated with LPS/IFN-γ (Figure 7, top panel, upper trace) generated small amounts of NO, utilizing internal arginine stores, and a steady-state level of approx. 1.15 μM was maintained following the addition of arginine. Addition of

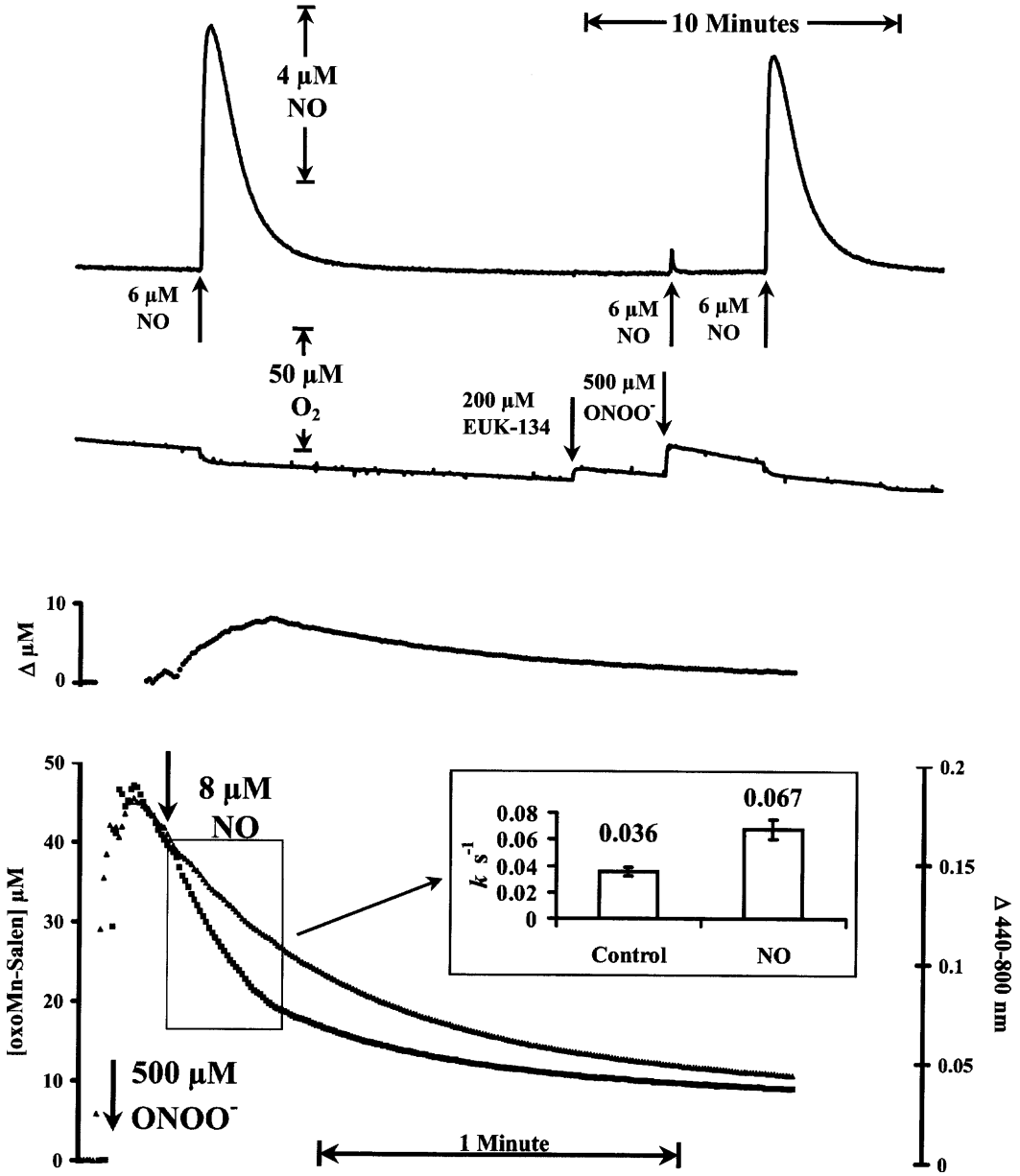

Figure 5 Effect of $ONOO^-$ and EUK-134 on NO

Top panel: a pair of NO and O_2 traces, recorded simultaneously, as in Figure 4. NO (6 nmol · ml^{-1}) was added and its slow decay was monitored. Following the decay of NO, EUK-134 was added, followed immediately by $ONOO^-$ at a final concentration of 500 μM. Some 10 s later (by which time the $ONOO^-$ would have decayed away) another aliquot of NO was added. Following the decay of this NO, a final aliquot of NO was added to the chamber. Bottom panel: shows the effect of 8 μM NO on the decay of oxoEUK-8, measured using the 440 minus 800 nm wavepair. In the lower traces, 500 μM $ONOO^-$ was added to 50 μM EUK-8 in 100 mM potassium phosphate/20 μM DTPA, pH 7.0. In the control trace (▲) the oxoEUK-8 was allowed to spontaneously decay. In the other trace (■) NO was added to a final concentration of 8 μM, where indicated by the arrow. The concentration of oxoEUK-8 was measured using an absorption coefficient of 4000 M^{-1} at Δ440–800 nm. The upper trace is the difference in oxoEUK-8, generated by subtracting the two lower traces. In this pair of traces the ratio of oxoEUK-8 consumption to NO added was approx. 1:1. The average stoichiometry was 0.84:1 ($n = 5$ for controls and NO addition experiments). The insert shows the average first-order decay rate of oxoEUK-8 ($\pm$S.D.) in controls (0.036 ± 0.0034) and experiments where 8 μM NO (0.067 ± 0.0074) was added ($n = 5$).

EUK-8 to a final concentration of 200 μM lowers the steady-state NO concentration to approx. 0.4 μM. Addition of the NO scavenger 2-(4-carboxyphenyl)-4,4,5,5-tetramethylimidazoline 1-oxyl 3-oxide (C-PTIO) to a concentration of 30 μM removed the final traces of NO.

The consumption of NO following the addition of EUK-8 reflected the steady-state level of H_2O_2 in the media, resulting mainly from the autoxidation of glucose [50]. Addition of 50 nM catalase instead of EUK-8 also resulted in a fall in the level of NO generated by activated astrocytes (similar to that observed by Brown [49]). Control experiments with cell media, in the presence and absence of cells, showed that these glucose-containing buffers contained levels of H_2O_2 in the low micromolar range.

Figure 7 (top panel, middle trace) shows the generation of NO by LPS/IFN-γ-treated astrocytes that had previously been exposed to EUK-8 in their growth medium. These cells were also capable of generating NO, but the steady-state level of NO

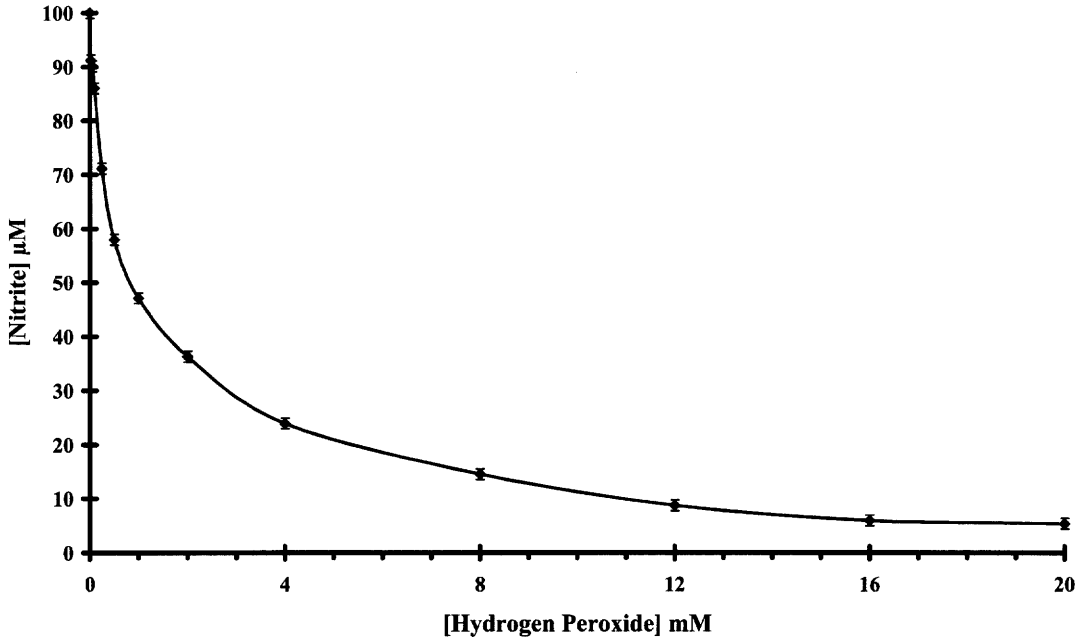

Figure 6 Effect of $ONOO^-$ and EUK-134 on NO_2^-

The effect of H_2O_2 concentration on the measurement of NO_2^-, in the presence of 200 μM EUK-134, after 30 min of incubation is shown. A 100 μl portion of 110 μM NO_2^- in 100 mM potassium phosphate/20 μM DTPA, pH 7.0, was aliquoted into a 96-well plate. 8×10 μl of various H_2O_2 solutions were added. After 30 min, 50 μl of 2% sulphanilamide in 5% HCl and 50 μl of 0.1% napthylethylenediamine was added. The plate was read at 540 nm, after 1 h incubation at room temperature. Each point represents data from eight wells, and the error bars show the S.D.

reached by these cells in the presence of arginine was only approx. 0.56 μM NO. Addition of EUK-8 to the external medium resulted in a fall in the NO steady state to approx. 0.16 μM, suggesting that the external medium had a lower steady-state level of H_2O_2.

The initial rates of NO production following the addition of arginine were 0.36 nmol of $NO \cdot mg^{-1} \cdot min^{-1}$ in the absence of EUK-8 and 0.15 nmol of $NO \cdot mg^{-1} \cdot min^{-1}$ in EUK-8-treated cells. However, as the rate of decay of NO in aqueous medium is proportional to $[NO]^2$ [51], it is difficult to estimate the rate of NO generation.

We wished to establish whether the EUK-8-treated cells were generating less NO than the controls or if the treated cells consumed NO at a greater rate, the latter argument being supported indirectly by the data in Figures 4 and 5. Astrocytes were incubated for 24 h in the presence and absence of 50 μM EUK-8, harvested, pelleted, re-suspended in respiration buffer and placed ($1 mg \cdot ml^{-1}$) in to a reaction chamber containing a NO electrode. NO was added to a final concentration of 2.5 μM and the decay of NO was monitored. Figure 7 (bottom panel) shows typical NO decay traces observed in the presence and absence of astrocytes, with or without EUK-8. NO decayed slowly in the respiration buffer; the arrow in Figure 7 (bottom panel) indicates the half-life of NO, which was approx. 75 s. NO decayed more quickly (half-life approx. 67 s) in the presence of untreated astrocytes, similar to the decay observed in mitochondria, liposomes and cells [52]. In the EUK-8-treated cells this half-life fell to only 32 s. This suggests that Mn-Salen, added to cell growth medium, remains associated with astrocytes following washing and is still capable of becoming oxidized to the corresponding oxo-species. We measured the decay of NO in the presence of cells grown for 24 h in the presence of both EUK-8 and EUK-134. The average half-life of 2.5 μM NO in $1 mg \cdot ml^{-1}$ control cells was 63 ± 4.7 s, whereas in EUK-8-treated astrocytes this half-life fell to 34 ± 4.9 s. In EUK-134-treated cells the rate of NO consumption was even higher, exhibiting a half-life of 9.1 ± 2.9 s ($n = 10$ in all cases). This difference between the EUK-8- and EUK-134-treated cells, with respect to the decay of NO, can be explained by the greater reactivity towards NO of oxoEUK-134, compared with oxoEUK-8.

We can estimate the rate of decay of NO at each of the steady-state levels observed in Figure 7 (top panel) from the data shown in Figure 7 (bottom panel). The rate of NO decay in control astrocytes at 1.15 μM NO was approx. 0.6 nmol of $NO \cdot min^{-1}$, very similar to the rate in EUK-8-treated astrocytes at 0.56 μM NO, approx. 0.53 nmol of $NO \cdot min^{-1}$. In a steady state, influx must match efflux, and so it appears that the rate at which NO is produced by the astrocytes is not altered by the presence of Mn-Salen, but that the rate of decay of NO is increased by treatment with Mn-Salen.

Measurement of NO_2^-/NO_3^- in Mn-Salen-treated astrocytic media and buffer

To confirm that Mn-Salen was not affecting the generation of NO, we measured the levels of NO_2^-/NO_3^- in astrocytic growth media incubated for 24 h in the presence or absence of EUK-8 or EUK-134 with or without LPS/IFN-γ, using nitrate reductase, and then measuring NO_2^- by the Griess assay. We found that the NO_3^- levels were approx. 30% less in Mn-Salen-treated cells compared with controls (results not shown). We found that even the low levels of Mn-Salen in the media were able to disrupt NO_3^- reductase and that low levels of oxoMn-Salen disrupted the V(III)-based method. Neither of these methods could be used to determine the NO_3^- in astrocytic media that had been treated with Mn-Salen. When the media from Mn-Salen-treated astrocytes were assayed for NO_2^-/NO_3^- using the chemiluminescence method, it was found that the total NO_2^-/NO_3^- levels were the

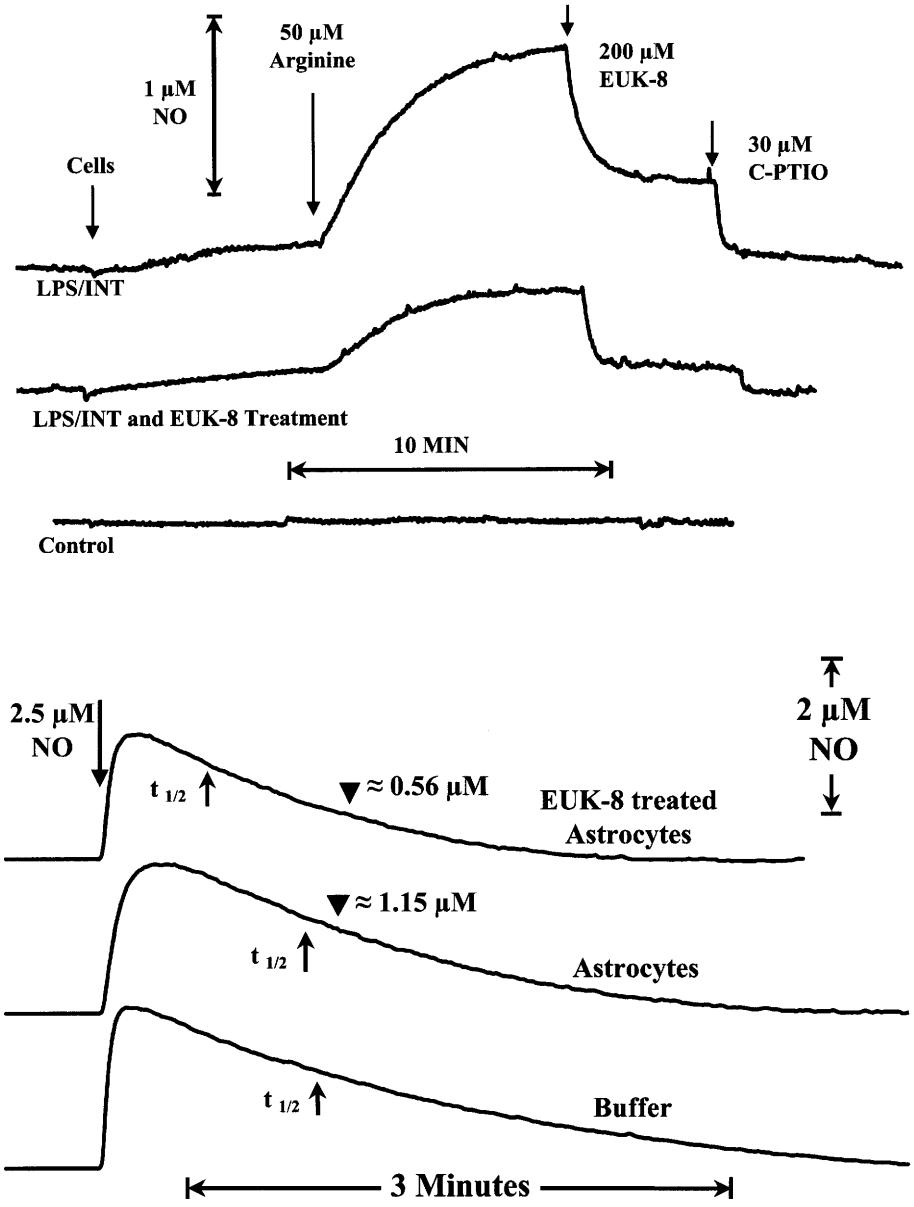

Figure 7 Effect of EUK-8-treated astrocytes on NO

Top panel: generation of NO by astrocytes treated with EUK-8 and inflammatory cytokines. Astrocytes (1 mg · ml^{-1} total protein) were placed in an incubation chamber containing respiration buffer (134 mM NaCl, 20 mM glucose, 20 mM Hepes, 5 mM KCl, 4 mM $NaHCO_3$, 2 mM $CaCl_2$, 0.43 mM KH_2PO_4 and 0.33 mM Na_2HPO_4, pH 7.4) and a NO electrode. The upper trace shows LPS/IFN-γ-treated astrocytes. Astrocytes generated small amounts of NO before the addition of 50 μM arginine, where the NO reached a steady-state level of approx. 1.15 μM. Addition of 200 μM EUK-8 lowered the steady-state level to 0.4 μM NO and addition of the NO scavenger C-PTIO removed the final traces of NO. The middle trace shows the generation of NO by LPS/IFN-γ + EUK-8-treated astrocytes. These cells generated a steady-state level of NO of approx. 0.56 μM NO. Addition of 200 μM EUK-8 lowered the steady-state level to 0.16 μM NO. The amount of NO generated by the control astrocytes was below the detection level of the NO electrode (approx. 10 nM). Bottom panel: typical decay profiles of NO in the presence of astrocytes. Astrocytes were incubated for 24 h in the absence or presence of 50 μM EUK-8 harvested and placed (1 mg · ml^{-1} total protein) into a reaction chamber containing a NO electrode. NO was added to a final concentration of 2.5 μM and the decay of NO was monitored. NO decayed slowly in the respiration buffer, the arrow (↑) indicating a half-life for NO of approx. 75 s. NO in the presence of untreated astrocytes had a half-life approx. 67 s. ▼ in the middle trace indicates the concentration of 1.15 μM NO. In EUK-8-treated cells this fell to only approx. 32 s; ▼ in the upper trace indicates the part of the trace where the concentration is 0.56 μM. The average half-life of 2.5 μM NO in the presence of 1 mg · ml^{-1} cells was 63 ± 4.7 s in control astrocytes, whereas in EUK-8-treated astrocytes this half-life fell to 34 ± 4.9 s ($P < 0.0005$, $n = 10$).

same as in the LPS/IFN-γ-treated astrocytes. This confirmed that Mn-Salen alters the decay, but not the formation rate, of NO in activated astrocytes.

DISCUSSION

Many disease states are associated with an overproduction of reactive oxygen species, OCl^-, O_2^- and H_2O_2, and/or reactive nitrogen species, NO and $ONOO^-$ [37]. We have demonstrated that Mn-Salens catalyse the removal of both OCl^- and $ONOO^-$ (Figure 2, bottom panel). In both cases the Mn-Salen is oxidized to the corresponding oxo-species via eqns (5) and (6).

$$Mn(III) + OCl^- \rightarrow Mn(V)O^{2-} + Cl^- \quad (5)$$

$$Mn(III) + ONOO^- \rightarrow Mn(V)O^{2-} + NO_2^- \quad (6)$$

Thus Mn-Salens, in the presence of inflammatory peroxy-compounds (H_2O_2, $ONOO^-$) and/or OCl^-, become oxidized to oxoMn-Salen and release benign species (H_2O, O_2, NO_2^- and Cl^-). In comparison with catalase, the Mn-Salens are poor catalysts of H_2O_2 breakdown, but oxoMn-Salens have interesting nitrogen chemistry. We have demonstrated that oxoMn-Salens consume NO (Figures 4 and 5). As oxoMn-Salens act as atomic-oxygen donor compounds [19] and in view of the aqueous chemistry of NO, it is likely that oxoMn-Salens oxidize NO to NO_2 (eqn 7). The inhibition of O_2 formation of oxoMn-Salens by NO and the stoichiometry of the reaction with the oxo-species of 0.67–0.84:1 supports this view. The NO_2 generated can then rapidly react with NO, producing N_2O_3 (eqn 8), which following hydration gives HNO_2 (eqn 9; see Wink et al. [51]). Given that NO_2 is generated during the normal process of NO autoxidation, and that it reacts rapidly with NO, *in vitro* and *in vivo*, it is unlikely that its generation by Mn-Salen from NO in disease states will prove deleterious.

$$Mn(V)O^{2-} + NO \rightarrow Mn(III) + NO_2 \quad (7)$$

$$NO_2 + NO \rightarrow N_2O_3 \quad (8)$$

$$N_2O_3 + H_2O \rightarrow 2HNO_2 \quad (9)$$

In addition, it was found that oxoMn-Salen complexes could also oxidize NO_2^- to NO_3^-. We found that NO_2^- was consumed at concentrations of H_2O_2 typical of those that are found in biological tissues [53]. The mechanism for this consumption of NO_2^- must be the oxidation of NO_2^- to NO_3^- (eqn 10).

$$Mn(V)O^{2-} + NO_2^- \rightarrow Mn(III) + NO_3^- \quad (10)$$

This oxidation of NO_2^- to NO_3^- and the interference with the nitrate reductase/V(III) methods for converting NO_3^- into NO_2^- means that great care must be exercised when measuring NO_2^-/NO_3^- in the presence of Mn-Salens and oxoMn-Salens.

It has been shown that Mn-Salens are useful agents in the treatment of disease states associated with oxidative stress [10–19]. We have demonstrated that Mn-Salen can be used to modulate the production of NO by activated astrocytes (Figure 7, top panel). The steady-state level of NO generated by Mn-Salen-treated astrocytes was some 2.5 times lower than in untreated cells. The difference in the steady-state levels of NO is due to the oxidation of NO by the Mn-Salen-treated astrocytes. The interference caused to the assays originally used to establish NO_2^-/NO_3^- levels in the astrocytic media initially suggested that Mn-Salens were altering the rate at which the astrocytes were generating NO. Close examination of the rates at which NO decayed in the presence of astrocytes, with or without Mn-Salen, demonstrates that only the NO decay rate was altered by Mn-Salen.

Mn-Salens may prove to be therapeutic agents where NO overproduction is a factor in pathophysiology, catalysing the oxidation of NO by H_2O_2, $ONOO^-$ or OCl^-. Many of the disease states that are associated with overproduction of NO have little effective treatment, e.g. sepsis. Sepsis can be most simply defined as a spectrum of clinical conditions caused by the immune response of a host to infection or trauma and characterized by systemic inflammation and coagulation [54]. It ranges from a systemic inflammatory response and organ dysfunction to multiple organ failure, and ultimately death for many patients. Antibiotic therapy and intensive physiological support continues to be the main approach to the management of patients with severe sepsis. Despite the development of numerous therapeutic agents, these drugs do little to improve patient outcome [55]. Mn-Salens might prove useful in treating sepsis, and rational drug design or compound screening will locate Mn-Salens with poor catalase activity but rapid oxidation to oxoMn-Salens, i.e. the reaction shown in eqn (3) is rapid, but that in eqn (4) is slow. This would result in a high level of oxoMn-Salen in the presence of oxidizing, inflammatory species (H_2O_2, OCl^- and $ONOO^-$). The oxoMn-Salens generated could then clear the body of a sepsis patient of excessive NO.

Now that we have elucidated the mechanisms by which Mn-Salens react with biological reactive nitrogen species, our data may help explain the actions of these compounds in the treatment of disease and in their ability to extend life spans.

We thank Professor Martin Hughes (Kings College London, London, U.K.) for his advice and suggestions, and Dr Charmaine Griffiths (The Wolfson Institute for Biomedical Research, University College London, London, U.K.) for the chemiluminesence determination of NO_2^-/NO_3^- levels. M.A.S. is supported by a fellowship from the Worshipful Company of Pewterers, City of London. V.C.S. was supported by the Brain Research Trust and also by the Hospital Savings Association. This work was funded by a grant to M.A.S. and J.B.C. from the Brain Research Trust.

REFERENCES

1 Harman, D. (1996) Aging and disease: extending functional life span. Ann. N.Y. Acad. Sci. **786**, 321–336
2 Gracy, R. W., Talent, J. M., Kong, Y. and Conrad, C. C. (1999) Reactive oxygen species: the unavoidable environmental insult? Mutat. Res. **428**, 17–22
3 Ku, H. H., Brunk, U. T. and Sohal, R. S. (1993) Relationship between mitochondrial superoxide and hydrogen peroxide production and longevity of mammalian species. Free Radical Biol. Med. **15**, 621–627
4 Ku, H. H. and Sohal, R. S. (1993) Comparison of mitochondrial pro-oxidant generation and anti-oxidant defences between rat and pigeon: possible basis of variation in longevity and metabolic potential. Mech. Ageing Dev. **72**, 67–76
5 Rogina, B. and Helfand, S. L. (2000) Cu, Zn superoxide dismutase deficiency accelerates the time course of an age-related marker in *Drosophila melanogaster*. Biogerontology **1**, 163–169
6 Griswold, C. M., Matthews, A. L., Bewley, K. E. and Mahaffey, J. W. (1993) Molecular characterisation and rescue of acatalasemic mutants of *Drosophila melanogaster*. Genetics **134**, 781–788
7 Sohal, R. S., Agarwal, A., Agarwal, S. and Orr, W. C. (1995) Simultaneous overexpression of copper- and zinc-containing superoxide dismutase and catalase retards age-related oxidative damage and increases metabolic potential in *Drosophila melanogaster*. J. Biol. Chem. **270**, 15671–15674
8 Baudry, M., Etienne, S., Bruce, A., Palucki, M., Jacobsen, E. and Malfroy, B. (1993) Salen-Manganese complexes are superoxide dismutase-mimics. Biochem. Biophys. Res. Commun. **192**, 964–968
9 Melov, S., Ravenscroft, J., Malik, S., Gill, M. S., Walker, D. W., Clayton, P. E., Wallace, D. C., Malfroy, B., Doctrow, S. R. and Lithgow, G. J. (2000) Extension of life-span with superoxide dismutase/catalase mimetics. Science **289**, 1567–1569
10 Bruce, A. J., Malfroy, B. and Baudry, M. (1996) Beta-Amyloid toxicity in organotypic hippocampal cultures: protection by EUK-8, a synthetic catalytic free radical scavenger. Proc. Natl. Acad. Sci. U.S.A. **93**, 2312–2316
11 Pong, K., Doctrow, S. R. and Baudry, M. (2000) Prevention of 1-methyl-4-phenylpyridinium- and 6-hydroxydopamine-induced nitration of tyrosine hydroxylase and neurotoxicity by EUK-134, a superoxide dismutase and catalase mimetic, in cultured dopaminergic neurons. Brain Res. **881**, 182–189
12 Baker, K., Marcus, C. B., Huffman, K., Kruk, H., Malfroy, B. and Doctrow, S. R. (1998) Synthetic combined superoxide dismutase/catalase mimics are protective as a delayed treatment in a rat stroke model: a key role for reactive oxygen species in ischemic brain injury. J. Pharmacol. Exp. Ther. **284**, 215–221
13 Jung, C. W., Rong, Y. Q., Doctrow, S., Baudry, M., Malfroy, B. and Xu, Z. S. (2001) Synthetic superoxide dismutase/catalase mimetics reduce oxidative stress and prolong survival in a mouse amyotrophic lateral sclerosis model. Neurosci. Lett. **304**, 157–160
14 Malfroy, B., Doctrow, S. R., Orr, P. L., Tocco, G., Fedoseyeva, E. V. and Benichou, G. (1997) Prevention and suppression of autoimmune encephalomyelitis by EUK-8, a synthetic catalytic scavenger of oxygen reactive metabolites. Cell. Immunol. **177**, 62–68
15 Rong, Y., Doctrow, S. R., Tocco, G. and Baudry, M. (1999) EUK-134, a synthetic superoxide dismutase and catalase mimetic, prevents oxidative stress and attenuates kainate-induced neuropathology. Proc. Natl. Acad. Sci. U.S.A. **96**, 9897–9902
16 Pucheu, S., Boucher, F., Sulpice, T., Tresallet, N., Bonhomme, Y., Malfroy, B. and deLeiris, J. (1996) EUK-8 a synthetic catalytic scavenger of reactive oxygen species protects isolated iron-overloaded rat heart from functional and structural damage induced by ischemia/reperfusion. Cardiovasc. Drugs Ther. **10**, 331–339

17 Gianello, P., Saliez, A., Bufkens, X., Pettinger, R., Misseleyn, D., Hori, S. and Malfroy, B. (1996) EUK-134, a synthetic superoxide dismutase and catalase mimetic, protects rat kidneys from ischemia-reperfusion-induced damage. Transplantation **62**, 1664–1666

18 Osman, R. and Basch, H. (1984) On the mechanism of action of superoxide-dismutase – a theoretical-study. J. Am. Chem. Soc. **106**, 5710–5714

19 Katsuki, T. (1995) Catalytic asymmetric oxidations using optically active (salen)manganese(III) complexes as catalysts. Coord. Chem. Rev. **140**, 189–214

20 Zhang, W. and Jacobsen, E. N. (1991) Asymmetric olefin epoxidation with sodium-hypochlorite catalyzed by easily prepared chiral Mn(III) Salen complexes. J. Org. Chem. **56**, 2296–2298

21 Carr, A. C. and Winterbourn, C. C. (1997) Oxidation of neutrophil glutathione and protein thiols by myeloperoxidase-derived hypochlorous acid. Biochem. J. **327**, 275–281

22 Kampf, C. and Roomans, G. M. (2001) Effects of hypochlorite on cultured respiratory epithelial cells. Free Radical Res. **35**, 499–511

23 Moncada, S., Palmer, R. M. J. and Higgs, E. A. (1991) Nitric oxide – physiology, pathophysiology, and pharmacology. Pharmacol. Rev. **43**, 109–142

24 Heales, S. J. R., Bolaños, J. P., Stewart, V. C., Brookes, P. S., Land, J. M. and Clark, J. B. (1999) Nitric oxide, mitochondria & neurological disease. Biochim. Biophys. Acta **1410**, 215–228

25 Huie, R. E. and Padmaja, S. (1993) The reaction of nitric oxide with superoxide. Free Radical Res. Commun. **18**, 195–199

26 Sharpe, M. A. and Cooper, C. E. (1998) Reactions of nitric oxide with mitochondrial cytochrome *c*: a novel mechanism for the formation of nitroxyl anion and peroxynitrite. Biochem. J. **332**, 9–19

27 Poderoso, J. J., Carreras, M. C., Schopfer, F., Lisdero, C. L., Riobo, N. A., Giulivi, C., Boveris, A. D., Boveris, A. and Cadenas, E. (1999) The reaction of nitric oxide with ubiquinol: kinetic properties and biological significance. Free Radical Biol. Med. **26**, 925–935

28 Uppu, R. M., Squadrito, G. L., Bolzan, R. M. and Pryor, W. A. (2000) Nitration and nitrosation by peroxynitrite: role of CO_2 and evidence for common intermediates. J. Am. Chem. Soc. **122**, 6911–6916

29 Radi, R., Beckman, J. S., Bush, K. and Freeman, B. A. (1991) Peroxynitrite oxidation of sulfhydryls: the cytotoxic potential of endothelial-derived superoxide and nitric oxide. J. Biol. Chem. **266**, 4244–4250

30 Pryor, W. A., Jin, X. and Squadrito, G. L. (1994) One and two electron oxidations of methionine by peroxynitrite. Proc. Natl. Acad. Sci. U.S.A. **91**, 11173–11177

31 Lehnig, M. (1999) L-tyrosine and related compounds as studied by N-15 chemically induced dynamic nuclear polarization. Arch. Biochem. Biophys. **368**, 303–318

32 Sloane, J. A., Hollander, W., Moss, M. B., Rosene, D. L. and Abraham, C. R. (1999) Increased microglial activation and protein nitration in white matter of the aging monkey. Neurobiol. Aging **20**, 395–405

33 Uttenthal, L. O., Alonso, D., Fernandez, A. P., Campbell, R. O., Moro, M. A., Leza, J. C., Lizasoain, I., Esteban, F. J., Barroso, J. B., Valderrama, R. et al. (1998) Neuronal and inducible nitric oxide synthase and nitrotyrosine immunoreactivities in the cerebral cortex of the aging rat. Microsc. Res. Tech. **43**, 75–88

34 Van der Loo, B., Labugger, R., Skepper, J. N., Bachschmid, M., Kilo, J., Powell, J. M., Palacios-Callender, M., Erusalimsky, J. D., Quaschning, T., Malinski, T. et al. (2000) Enhanced peroxynitrite formation is associated with vascular aging. J. Exp. Med. **192**, 1731–1743

35 Tohgi, H., Abe, T., Yamazaki, K., Murata, T., Ishizaki, E. and Isobe, C. (1999) Alterations of 3-nitrotyrosine concentration in the cerebrospinal fluid during aging and in patients with Alzheimer's disease. Neurosci. Lett. **269**, 52–54

36 Kasapoglu, M. and Özben, T. (2001) Alterations of antioxidant enzymes and oxidative stress markers in aging. Exp. Geront. **36**, 209–220

37 Sayre, L. M., Smith, M. A. and Perry, G. (2001) Chemistry and biochemistry of oxidative stress in neurodegenerative disease. Curr. Med. Chem. **8**, 721–738

38 Law, A., Gauthier, S. and Quirion, R. (2001) Say NO to Alzheimer's disease: the putative links between nitric oxide and dementia of the Alzheimer's type. Brain Res. Rev. **35**, 75–96

39 Ferrante, R. J., Hantraye, P., Brouillet, E. and Beal, M. F. (1999) Increased nitrotyrosine immunoreactivity in substantia nigra neurons in MPTP treated baboons is blocked by inhibition of neuronal nitric oxide synthase. Brain Res. **823**, 177–182

40 Eliasson, M. J. L., Huang, Z. H., Ferrante, R. J., Sasamata, M., Molliver, M. E., Snyder, S. H. and Moskowitz, M. A. (1999) Neuronal nitric oxide synthase activation and peroxynitrite formation in ischemic stroke linked to neural damage. J. Neurosci. **19**, 5910–5918

41 Sasaki, S., Shibata, N., Komori, T. and Iwata, M. (2000) iNOS and nitrotyrosine immunoreactivity in amyotrophic lateral sclerosis. Neurosci. Lett. **291**, 44–48

42 Oleszak, E. L., Zaczynska, E., Bhattacharjee, M., Butunoi, C., Legido, A. and Katsetos, C. D. (1998) Inducible nitric oxide synthase and nitrotyrosine are found in monocytes/macrophages and/or astrocytes in acute, but not in chronic, multiple sclerosis. Clin. Diag. Lab. Immunol. **5**, 438–445

43 Boucher, L. J. (1973) Manganese Schiff's base complexes-II. J. Inorg. Nuclear Chem. **35**, 3731–3738

44 Boucher, L. J. and Farrell, M. O. (1973) Manganese Schiff's base complexes-I. J. Inorg. Nuclear Chem. **36**, 531–536

45 Green, L. C., Wagner, D. A., Glogowski, J., Skipper, P. L., Wishnok, J. S. and Tannenbaum, S. R. (1982) Analysis of nitrate, nitrite, and [N-15]-labelled nitrate in biological-fluids. Anal. Biochem. **126**, 131–138

46 Miranda, K. M., Espey, M. G. and Wink, D. A. (2001) A rapid, simple spectrophotometric method for simultaneous detection of nitrate and nitrite. NO Biol. Chem. **5**, 62–71

47 Uppu, R. M. and Pryor, W. A. (1996) Synthesis of peroxynitrite in a two-phase system using isoamyl nitrite and hydrogen peroxide. Anal. Biochem. **236**, 242–249

48 Bolaños, J. P., Peuchen, S., Heales, S. J. R., Land, J. M. and Clark, J. B. (1994) Nitric oxide-mediated inhibition of the mitochondrial respiratory chain in cultured astrocytes. J. Neurochem. **63**, 910–916

49 Brown, G. C. (1995) Reversible binding and inhibition of catalase by nitric oxide. Eur. J. Biochem. **232**, 188–191

50 Horowitz, P. M., Butler, M. and McClure, G. D. (1992) Reducing sugars can induce the oxidative inactivation of rhodanese. J. Biol. Chem. **267**, 23596–23600

51 Wink, D. A., Darbyshire, J. F., Nims, R. W., Saavedra, J. E. and Ford, P. C. (1993) Autoxidation kinetics of aqueous nitric-oxide. Chem. Res. Toxicol. **6**, 23–27

52 Thomas, D. D., Liu, X., Knatrow, S. P. and Lancaster, J. R. (2001) The biological lifetime of nitric oxide: implications for the perivascular dynamics of NO and O_2. Proc. Natl. Acad. Sci. U.S.A. **98**, 355–360

53 Chance, B., Sies, H. and Boveris, A. (1979) Hypoperoxide metabolism in mammalian organs. Physiol. Rev. **59**, 527–605

54 Wheeler, A. P. and Bernard, G. R. (1999) Treating patients with severe sepsis. N. Engl. J. Med. **340**, 207–214

55 Marik, P. E. and Varon, J. (1998) The management of sepsis: A practical review. J. Int. Care Med. **13**, 229–240

Received 24 January 2002/4 April 2002; accepted 7 May 2002
Published as BJ Immediate Publication 7 May 2002, DOI 10.1042/BJ20020154